Articles

Characterization of the Surfactin Synthetase C-Terminal Thioesterase Domain as a Cyclic Depsipeptide Synthase†

Claire C. Tseng,‡,§ Steven D. Bruner,§ Rahul M. Kohli,§ Mohamed A. Marahiel,|| Christopher T. Walsh,*,§ and Stephan A. Sieber‡,§,||

Department of Biological Chemistry and Molecular Pharmacology, Harvard Medical School, 240 Longwood Avenue, Boston, Massachusetts 02115, and Fachbereich Chemie, Philipps-Universität Marburg, Hans-Meerwein-Strasse, 35032 Marburg, Germany

Received August 7, 2002

ABSTRACT: The C-terminal thioesterase domain of the nonribosomal peptide synthetase producing the lipopetide surfactin (Srf TE) retains autonomous ability to generate the cyclic peptidolactone skeleton of surfactin when provided with a soluble β-hydroxy-butyryl-heptapeptidyl thioester substrate. Utilizing the recently solved crystal structure [Bruner, S. D., et al. (2002) *Structure 10*, 301−310], the active-site nucleophile, Ser80, was changed to Cys, and the other members of the catalytic triad, Asp107 and His207, were changed to Ala, with the resulting mutants lacking detectable activity. Two cationic side chains in the active site, Lys111 and Arg120, were changed to Ala, causing an increased partitioning of the product to hydrolysis, as did a P26G mutant, mimicking the behavior of lipases. To evaluate recognition elements in substrates used by Srf TE, alterations to the fatty acyl group, the heptapeptide, and the thioester leaving group were made, and the resulting substrates were characterized for kinetic competency and flux of product to cyclization or hydrolysis. Alterations that could be accepted for cyclization were identified in all three parts of the substrate, although tolerance limits for changes varied. In addition, cocrystal structures of Srf TE with dipeptidyl boronate inhibitors were solved, illustrating the critical binding determinants of the substrate. On the basis of the structures and biochemical data, the cyclizing conformation of the surfactin peptide was modeled into the enzyme active site.

Macrocyclic natural products produced by nonribosomal peptide synthetases (NRPSs)[1] and polyketide synthases (PKSs), such as tyrocidine, ramoplanin, daptomycin, erythromycin, iturin, and surfactin, display a wide variety of antibiotic and antitumor activities (Figure 1). The macrocyclic structure of these compounds reduces conformational flexibility, ordering the biologically active conformation, and contributes to stability against proteolytic enzymes, an important property for pharmacological applications (*1*, *2*). NRPSs utilize various cyclization strategies to increase product diversity. For example, the cycle can be a peptidolactam as in tyrocidine, or a branched chain lipodepsipeptide as in ramoplanin, daptomycin, and surfactin. In daptomycin and ramoplanin, the lactone ring forms between the carbonyl of the C-terminal residue and a natural or nonnatural amino acid side chain, threonine or β-hydroxy-asparagine, respectively. On the other hand, in surfactin and iturin, a β-hydroxyl (surfactin) or β-amino (iturin) fatty acid acts as the nucleophile to form a lactone or lactam, respectively. An important feature of cyclic peptides is the β-sheet content, which is high for molecules with $(4n + 2)$ residues (*1*, *3*). A peptide with high β-sheet content facilitates cyclization through substrate preorganization, and is also thought to be involved in target-ligand binding (*4*, *5*).

Surfactin is a lipoheptapeptide produced by the gram positive bacterium *Bacillus subtilis* (*5*). Its primary sequence is FA-Glu-Leu-D-Leu-Val-Asp-D-Leu-Leu, where FA is a β-hydroxy $C_{13}-C_{15}$ fatty acid (Figure 1). The molecule is cyclized through the formation of an ester bond between the hydroxyl group of the fatty acid and the carbonyl of the C-terminal Leu. In addition to the exceptional surfactant power provided by its amphiphilic sequence, surfactin has been reported to exhibit hemolytic, antivirial, antibacterial, and antitumor properties (reviewed in ref *5*).

The biosynthesis of surfactin is achieved by the surfactin NRPS, which consists of three protein subunits, SrfA (402

† This work was supported by NIH Grant GM 20011 (C.T.W.) and Deutsche Forschungsgemeinschaft (M.A.M.). S.A.S. was supported by the Studienstiftung des deutschen Volkes, C.C.T. by a National Defense Science and Engineering Graduate Fellowship, S.D.B. by the Cancer Research Fund of the Damon Runyon-Walter Winchell Foundation, and R.M.K. by the Medical Scientist Training Program.

* To whom correspondence should be addressed.

‡ These authors contributed equally to this work.

§ Harvard Medical School.

|| Philipps-Universität Marburg.

[1] Abbreviations: NRPS, nonribosomal peptide synthetase; PKS, polyketide synthase; FAS, fatty acid synthase; TE, thioesterase domain; SNAC, *N*-acetylcysteamine; ONAC, *N*-acetylethanolamine, NNAC, *N*-acetylethylenediamine; Dap, 2,3-diaminopropionic acid; Ahx, ϵ-aminohexanoic acid.

10.1021/bi026592a CCC: $22.00
Published on Web 10/15/2002

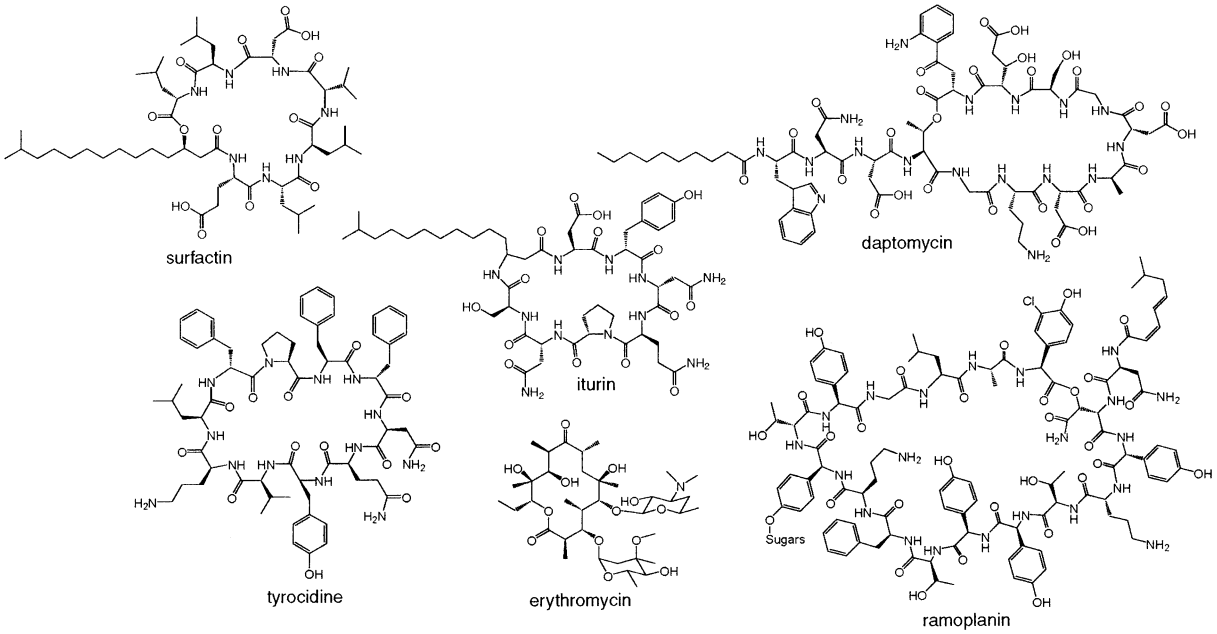

FIGURE 1: Structures of cyclic natural products from NRPS (surfactin, daptomycin, iturin, ramoplanin, and tyrocidine) and PKS (erythromycin) systems.

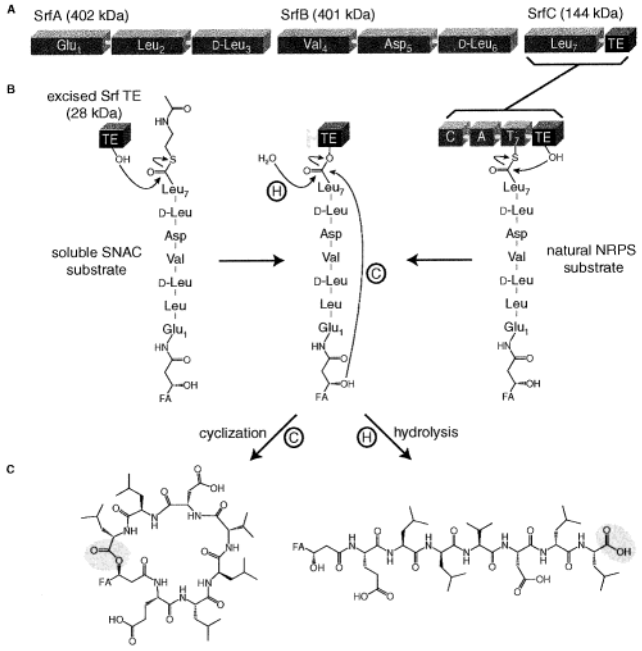

FIGURE 2: Schematic diagram of the surfactin NRPS and a close-up of the mechanism of catalysis by Srf TE. (A) Surfactin NRPS. Large boxes represent modules; each is labeled with the amino acid it incorporates. (B) TE domain mechanism. Small boxes represent protein domains; OH represents the TE active-site serine. In the native NRPS system, the peptidyl-*O*-TE acyl enyzme intermediate is formed by transfer of the peptidyl chain from the terminal T domain (T_7) to the active-site serine. In the model system used in this study, an excised Srf TE is used, and a soluble SNAC thioester substrate replaces the natural peptidyl-*S*-T domain substrate. The acyl enzyme intermediate is resolved through capture either by the β-hydroxy group of the fatty acid moiety, leading to cyclization, or by water, leading to hydrolysis. (C) Structures of the cyclic and hydrolyzed products of Srf TE catalysis.

kDa), SrfB (401 kDa), and SrfC (144 kDa) (Figure 2A) (*6*). In the surfactin assembly line, seven modules responsible for the incorporation of the seven amino acids in the peptide sequence are distributed 3/3/1 across the three subunits. Each module consists of several catalytic core domains responsible for recognition, activation, transfer, and condensation of a dedicated amino acid (Figure 2B), with peptide synthesis proceeding by a "multiple carrier thiotemplate mechanism" (*7*). According to this mechanism, a module first activates and covalently tethers (A domain) a specific amino acid via a thioester linkage (*S*-pantetheinyl chain of T domain). Each module then connects its amino acid to the molecule on the previous module through formation of an amide bond and concomitant cleavage of the previous thioester linkage (C domain), thus translocating a growing linear peptide from one module to the next.

Cyclization and release of the surfactin lipoheptapeptide chain from the enzyme is mediated by a 28 kDa thioesterase (TE) domain (Srf TE) embedded at the downstream end of the final subunit, SrfC (Figure 2A). Previous investigations with an excised Srf TE showed that it is active in vitro, and initial experiments indicated that the enzyme accepts soluble peptidyl-*S*-*N*-acetylcysteamine (peptidyl-SNAC) thioester substrates as mimics for the natural interaction with the peptidyl-*S*-T domain (Figure 2B) (*1*). Crystallographic data of Srf TE showed that it is a member of the α,β-hydrolase enzyme family, and structural similarity to serine esterases suggested that an active-site catalytic triad is responsible for the enzyme's macrocyclizing chain termination activity (*8*). According to a model based on the structure, the peptidyl chain bound to the adjacent T_7 domain is directed through a cleft into the active site of the TE domain and transferred onto an invariant serine residue (Ser80), which is activated by histidine (His207) and aspartate (Asp107) (Figure 2B). The peptidyl chain of this peptidyl-*O*-TE acyl enzyme intermediate is accommodated in a predominantly hydrophobic binding pocket with two cationic residues (Lys111 and Arg120) predicted to direct cyclization through specific interactions with the substrate (Figure 10A). In the deacylation half reaction, the β-hydroxyl group of the fatty acid moiety, activated by the same histidine and aspartate, forms the lactone by intramolecular nucleophilic attack on the acyl-

enzyme ester bond. Alternatively, as observed in other NRPS, PKS, and fatty acid synthase (FAS) TE domains, water can be a competing nucleophile, leading to linear acid products (Figure 2, panels B and C).

It has remained unclear what features direct the acyl-*O*-TE intermediates between cyclization and hydrolysis. To address this question, we have used the Srf TE structural information to assess residues that may be involved in kinetic- and/or product-determining steps. We have also begun an evaluation of the catalytic capacity of Srf TE to process surrogate substrates altered in the fatty acyl, peptidyl, or thioester leaving groups for both cyclization and hydrolysis.

EXPERIMENTAL PROCEDURES

Site-Directed Mutagenesis. Srf TE was cloned, expressed, and purified as previously described (*1*). The gene fragments encoding the Srf TE mutants were constructed using the QuickChange site directed mutagenesis kit (Stratagene). Constructs were obtained by PCR amplification of the Srf TE-containing pQE60 plasmid (*1*) with the following oligonucleotides (modified sequences underlined): **P26G**, 5′-ATT TTC GCA TTT CCG GGG GTC TTG GGC TAT GGC CT-3′ and 5′-AGG CCA TAG CCC AAG ACC CCC GGA AAT GCG AAA AT-3′; **S80C**, 5′-CAT TGT TTG GAT ATT GCG CGG GAT GCA GCC TGG CG-3′ and 5′-CGC CAG GCT GCA TCC CGC GCA ATA TCC AAA CAA TG-3′; **D107A**, 5′-GCG GAT CAT CAT GGT CGC TTC CTA TAA AAA ACA AGG TGT C-3′ and 5′-GAC ACC TTG TTT TTT ATA GGA AGC GAC CAT GAT GAT CCG C-3′; **K111A**, 5′-GGT CGA TTC CTA TAA AGC ACA AGG TGT CAG TGA TCT GG-3′ and 5′-CCA GAT GAC TGA CAC CTT GTG CTT GTG CTT TAT AGG AAT CGA CC-3′; **R120A**, 5′-TGT CAG TGA TCT GGA CGG AGC CAC GGT TGA AAG TGA-3′ and 5′-TCA CTT TCA ACC GTG GCT CCG TCC AGA TCA CTG ACA-3′; **H207A**, 5′-AAG AGG CTT CGG AAC AGC CGC AGA AAT GCT GCA GG-3′ and 5′-CCT GCA TTT CTG CGG CTG TTC CGA AGC CTC TT-3′. *Escherichia coli* XL1 Blue (Stratagene) was used for preparation of recombinant plasmids. Mutagenesis products were confirmed by sequencing with an ABI Prism 310 (Applied Biosystems).

Overexpression and Purification. Overproduction of recombinant hexahistidine-tagged proteins was carried out in *E. coli* M15 using standard protocols. The expressed proteins were purified by Ni-NTA chromatography and dialyzed into standard buffer (25 mM HEPES, 50 mM NaCl, pH 7.0). All proteins were flash frozen in liquid nitrogen and could be stored at −80 °C over several months without measurable loss of activity. Concentrations of purified proteins were determined spectrophotometrically using estimated extinction coefficients at 280 nm.

Synthesis of Peptidyl-SNAC Thioester Substrates. Peptide thioester substrate production and purification was carried out as described previously (*1*, *9*). Protected amino acids were purchased from Novabiochem, except for Fmoc-Dap(Boc)-OH and Fmoc-D-Dap(Boc)-OH (Bachem Bioscience). All other compounds were purchased from Sigma-Aldrich, except for *N*-acetylethanolamine (ONAC) (Tokyo Kasei Kogyo) and (*R*)-*N*-Boc-3-aminobutyric acid (Tyger Scientific). The identities of peptidyl-SNAC thioesters were verified by liquid chromatography−mass spectrometry (LC-MS) and matrix-assisted laser desorption ionization-time-of-flight (MALDI-TOF) MS (Table 1).

Table 1: Characterization of Substrates and Reaction Products by MS

		observed mass (calculated mass) (Da)		
peptide	species	substrate	cyclized product	hydrolyzed product
SLP-wt	$[M - H]^-$	999.7 (999.5)	880.7 (880.5)	898.6 (898.5)
SLP-1	$[M + H]^+$	959.4 (958.6)	N/D[a]	857.4 (857.5)
SLP-2	$[M + H]^+$	973.9 (974.5)	855.5 (855.5)	873.5 (873.5)
SLP-3	$[M + H]^+$	974.8 (974.5)	854.9 (855.5)	873.0 (873.5)
SLP-4	$[M + H]^+$	989.1 (988.5)	869.6 (869.5)	887.6 (887.5)
SLP-5	$[M + H]^+$	972.3 (972.6)	853.0 (853.5)	871.0 (871.5)
SLP-6	$[M + H]^+$	974.4 (974.5)	N/D	N/D
SLP-7	$[M + H]^+$	974.1 (974.5)	N/D	N/D
SLP-1/2	$[M + H]^+$	871.9 (872.5)	752.8 (753.5)	771.0 (771.5)
SLP-3/4	$[M + H]^+$	901.8 (902.5)	783.3 (783.4)	800.8 (801.5)
SLP-5/6	$[M + H]^+$	885.9 (886.5)	767.0 (767.5)	785.0 (785.5)
SLP-wt cycle	$[M - H]^-$	880.7 (880.5)	N/A[b]	898.1 (898.5)
SLP−ONAC	$[M - H]^-$	983.8 (983.5)	880.6 (880.5)	898.6 (898.5)
SLP-ϵOH	$[M + H]^+$	1002.6 (1002.5)	883.5 (883.5)	901.5 (901.5)

[a] N/D = product not detected. [b] N/A = not applicable.

Assays. Reactions were carried out in 25 mM MOPS, pH 7.0, in a total volume of 50 μL. Substrate concentration was 250 μM for standard reactions and varied for kinetic investigations. For the cycle opening reactions, 250 mM of SNAC, ONAC, or *N*-acetylethylenediamine (NNAC) was added. Reactions were initiated by addition of enzyme to give a final concentration of 2.5 μM for standard reactions and 2.0 μM for kinetic studies. Reactions were quenched by addition of 35 μL of 4% TFA/H_2O, and the products were analyzed by analytical HPLC (Beckman Coulter System Gold) with a reversed-phase (C_{18}) column (Vydac). Different gradients were applied according to resolution and solubility of the substrates (typically 0−35 min, 20 to 100% B, or 0−45 min, 0 to 70% B; A = H_2O, 0.1% TFA; B = acetonitrile; 1 mL/min). Concentrations of peptidyl-SNAC thioesters were calculated using experimentally determined extinction coefficients at 220 nm and assumed to be the same for the cyclized and hydrolyzed products. Kinetic characterization of the cyclization and hydrolysis reactions were carried out by determining initial rates at 5−10 substrate concentrations, using two to three time points at each concentration. The identities of products were confirmed by LC-MS and MALDI-TOF MS (Table 1), and the cyclic product of **SLP-ϵOH** was additionally verified by HPLC MS-MS analysis.

Enzymatic Synthesis of the Cyclic Macrolactone. The preparative scale synthesis of cyclic **SLP-wt** was carried out under standard assay conditions in a total volume of 10 mL. After 2.5 h, the reaction was quenched with 500 μL of TFA and centrifuged at 2000 rpm for 5 min. The supernatant was lyophylized overnight and redissolved in 2 mL of 1:1 H_2O/acetonitrile. The cycle was isolated by preparative HPLC with a reversed-phase (C_{18}) column (Vydac). Cyclic **SLP-wt** elutes at 24 min (10 mL/min; 0−35 min, 20 to 100% B; A = H_2O, 0.1% TFA; B = acetonitrile).

Cocrystallization with Boronic Acid Inhibitors. Peptide boronic acids were synthesized using established procedures (*10*, *11*). Crystals of Srf TE were grown as described, using 100 mM HEPES, pH 7.5, 1.8 M ammonium sulfate, and 2% MPD as precipitant (*8*). Crystals were transferred into buffer

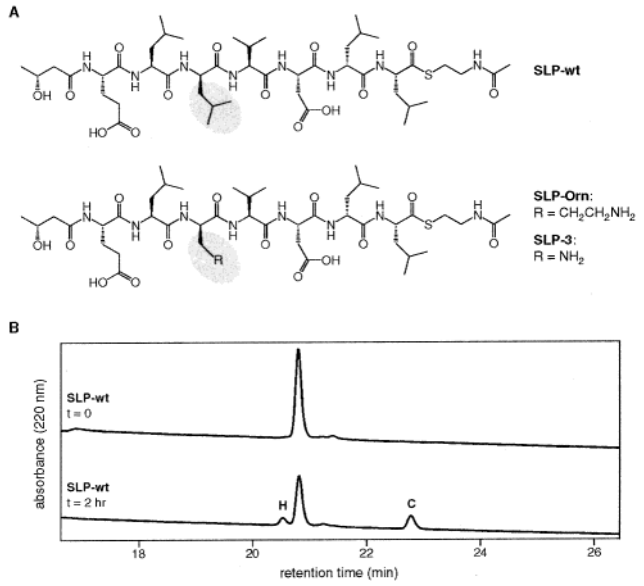

FIGURE 3: Cyclization and hydrolysis of a peptide-SNAC thioester substrate by Srf TE. (A) Structures of **SLP-wt**, **SLP−Orn**, and **SLP-3**. (B) HPLC traces of 2 h reaction initially containing 2.5 μM Srf TE, 250 μM **SLP-wt**, and 25 mM MOPS, at pH 7.0 and 24 °C. The peaks corresponding to the cyclic (C) and hydrolyzed (H) products are labeled. The identities of the substrate and products were verified by MALDI-TOF MS (Table 1).

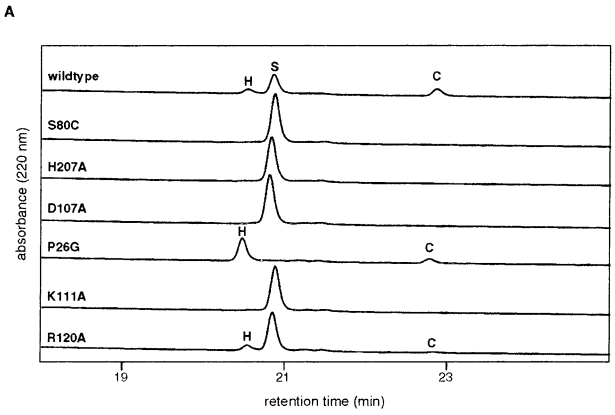

B

	k_{cat}/K_M for **SLP-wt** (mM^{-1} min^{-1})		**SLP-wt** C/H ratio	k_{cat}/K_M for **SLP-3** (mM^{-1} min^{-1})		**SLP-3** C/H ratio
	cyclization	hydrolysis		cyclization	hydrolysis	
wildtype	0.86	0.35	2.5	2.9	5.4	0.54
S80C	N/D	N/D	---	N/D	N/D	---
D107A	N/D	N/D	---	N/D	N/D	---
H207A	N/D	N/D	---	N/D	N/D	---
P26G	3.7	12	0.31	0.30	11	0.027
K111A	N/D	N/D	---	N/D	0.61	---
R120A	0.078	0.40	0.20	2.1	10	0.21

FIGURE 4: Characterization of Srf TE mutants. (A) HPLC traces of 2 h reactions initially containing 2.5 μM indicated enzyme, 250 μM **SLP-wt**, and 25 mM MOPS, at pH 7.0 and 24 °C. The peaks corresponding to the cyclic (C) and hydrolyzed (H) products and substrate (S) are labeled. (B) The ratio of cyclization to hydrolysis (C/H ratio), and k_{cat}/K_M values of cyclization and hydrolysis, for each mutant with **SLP-wt** and **SLP-3** (standard deviation ± 10%). N/D = activity not detected.

containing the peptide boronic acid and cryoprotectant (100 mM HEPES, pH 7.5, 2 M ammonium sulfate, 2% ethylene glycol monomethyl ether, 20% PEG 400, and 0.5 mM peptide boronic acid inhibitor), and soaked for 48 h at 22 °C. Crystals were frozen in liquid nitrogen and diffraction data collected on a Bruker SMART APEX home source X-ray system. Cocrystals of *N*-Ac-D-Leu-Leu-B(OH)$_2$ and the TE domain diffracted to a resolution of 2.1 Å with data at 98.3% completeness and an R_{merge} of 6.6%. Structures were solved by molecular replacement using the structure of unliganded Srf TE (PDB code = 1jmk) as a search model (R_{free} = 27.1%, $R_{working}$ = 23.5%).

RESULTS

Native SNAC Substrate. We previously reported that Srf TE catalyzed the stereospecific cyclization of a linear surfactin precursor peptidyl-SNAC thioester that was a mimic of the acylheptapeptide sequence of authentic surfactin (*1*). To improve water solubility, the sequence of this substrate differed from that of the wild-type substrate in that D-ornithine replaced D-Leu$_3$ and (*R*)-3-hydroxybutyric acid replaced the β-hydroxy $C_{13}-C_{15}$ fatty acid (**SLP−Orn**, Figure 3A). Reactions of **SLP−Orn** with Srf TE, in the presence of 1% glycerol as an enzyme stabilizer, produced a 1:1:1 ratio of the products of cyclization, hydrolysis, and glycerolysis, with similar k_{cat} (15−22 min^{-1}) and K_M (4.0−5.6 mM) values for all three products (*1*).

To establish a baseline using a substrate more similar to the wild-type substrate, a peptidyl-SNAC thioester was synthesized that included the native heptapeptide sequence, but retained the β-hydroxy-C_4 fatty acid substitution of **SLP−Orn** (**SLP-wt**, Figure 3A). **SLP-wt** was soluble in water to 2 mM, and in DMSO to 50 mM. Reactions of **SLP-wt** (250 μM, 0.5% DMSO, 25 mM MOPS, pH 7.0) with Srf TE (2 μM) in the absence of glycerol produced a 2.5:1 ratio of the cyclic:hydrolyzed products, with a k_{cat}/K_M of 0.86 mM^{-1} min^{-1} for cyclization and 0.35 mM^{-1} min^{-1} for hydrolysis (Figure 3B). The k_{cat} and K_M values could not be deconvoluted, because K_M concentrations of substrate could not be reached due to the low solubility of **SLP-wt** in water. These solubility limitations are expected to be exacerbated with the $C_{13}-C_{15}$ acyl chains in the wild-type heptapeptide sequence of surfactin. Nonetheless, product analysis of **SLP-wt** showed that Srf TE could direct about 70% of the flux of β-hydroxy-acyl-heptapeptidyl-*O*-enzyme intermediate to the macrolactone ring of the natural product.

Srf TE Mutants. Six point mutations were individually introduced into Srf TE based on analysis of the crystal structure (*8*). The presumed catalytic serine, Ser80, was changed to cysteine, and the other two residues of the proposed catalytic triad, Asp107 and His207, were each changed to alanine. These mutants were all inactive with **SLP-wt** as substrate, indicating that all three residues are critical for enzymatic activity and can indeed be ascribed to a catalytic triad (slight hydrolysis activity was observed with the D107A mutant in overnight incubations) (Figure 4). Two prominently placed basic residues in the largely hydrophobic active site of Srf TE, Lys111 and Arg120, were each changed to alanine. The K111A mutant was inactive on **SLP-wt** (slight hydrolysis activity was observed in overnight incubations), while the R120A mutant catalyzed the formation of decreased levels of the cyclized product (Figure 4). In comparison with the wild-type Srf TE, the R120A mutant showed an 11-fold decrease in k_{cat}/K_M for cyclization (0.078 mM^{-1} min^{-1}), and a comparable k_{cat}/K_M for hydrolysis (0.40 mM^{-1} min^{-1}).

A P26G mutant was made based on the sequence alignment of Srf TE with other TE domains and lipases (data not shown), other members of the α,β-hydrolase enzyme family that catalyze only hydrolysis of ester/lactone substrates (*12*). A proline conserved among TE domains, Pro26 in Srf TE, is instead conserved as a glycine in lipases, and the position of this residue near those responsible for the formation of the oxyanion hole in the active site (Val27 and Ala81) indicates that it may have an effect on product-determining catalysis of cyclization vs hydrolysis by the enzyme (Figure 10A). Indeed, reactions of **SLP-wt** with the P26G mutant produced two observations of note. One was a 12-fold change in product ratio to favor hydrolysis, down to a cyclization:hydrolysis ratio of 0.2:1 (Figure 4B). The other was a net increase in catalytic flux to 15.7 mM^{-1} min^{-1}, up from 1.2 mM^{-1} min^{-1} in wild-type Srf TE; of this 13-fold increase in overall flux, 80% of **SLP-wt** underwent hydrolysis.

Dap Scan of Heptapeptide Sequence. To evaluate recognition elements in the heptapeptidyl substrate chain and improve its limiting solubility, a systematic alteration of each of the side chains of the substrate was considered. We anticipated that an alanine scan would not improve the hydrophobic constraints on solubility; instead, a 2,3-diaminopropionic acid (Dap) residue with an ionizable 3-amino group was introduced at each of the seven residue positions of **SLP-wt**, with the stereochemistry of each residue maintained (Figure 5A). The resulting seven peptides, **SLP-1** to **SLP-7**, were assessed as substrates for Srf TE by determining the kinetic parameters and cyclization:hydrolysis ratio of Srf TE on each substrate, with the results summarized in Figure 5C. The solubilities of the Dap-containing substrates in water were much improved (25−50 mM) over **SLP-wt**, except when the Dap replaced an acidic residue, as in **SLP-1** and **SLP-5**, which displayed solubility properties similar to **SLP-wt**. However, separate k_{cat} and K_M values could still not be measured for those substrates with improved solubility, because severe substrate inhibition was observed at concentrations greater than 3 mM. This inhibition could be related to the critical micellar concentration of these substrates (*13*), which were measured to be in the 0.6−2.0 mM range (data not shown).

Nonetheless, the Dap scan allowed us to determine which residues were tolerant to a significant change of both size and charge. The residues in the middle of the substrate (Leu_2, D-Leu_3, Val_4, and Asp_5) were tolerant to Dap substitution to varying degrees, with each forming measurable amounts of both cyclized and hydrolyzed products (Figure 5). On the other hand, the residues adjacent to either (1) the site of acyl−enzyme intermediate formation at the C-terminus of the substrate (D-Leu_6 and Leu_7), or (2) the fatty acid containing the nucleophile for cyclization (Glu_1), were not tolerant to the change (Figure 5). Dap substitution at D-Leu_6 or Leu_7 resulted in a substrate that could be neither cyclized nor hydrolyzed (**SLP-6**/**SLP-7**), indicating that these residues are critical to recognition of the substrate by the enzyme for acyl−enzyme intermediate formation. In contrast, substitution at Glu_1 resulted in a substrate that could be hydrolyzed but not cyclized (**SLP-1**), suggesting that this residue is important for attack by the internal nucleophile to cyclize the acyl−enzyme intermediate.

Unexpectedly, the k_{cat}/K_M of Srf TE for the cyclization of **SLP-3** was almost four times greater than that for **SLP-wt**,

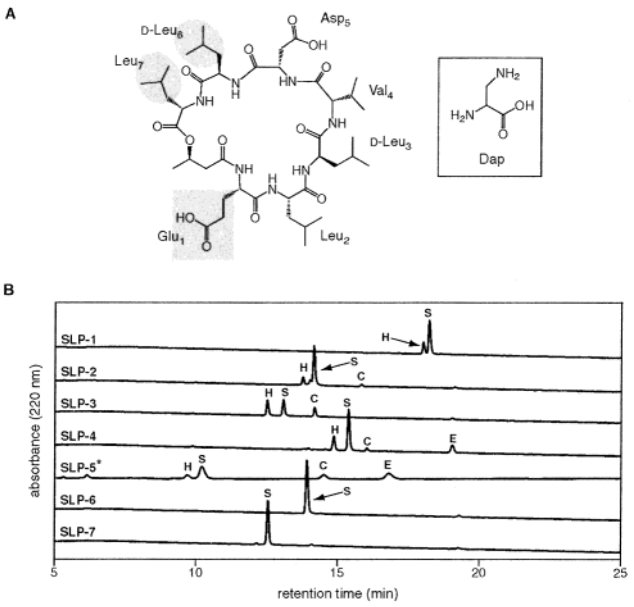

C

	k_{cat}/K_M for cyclization ($mM^{-1}min^{-1}$)	k_{cat}/K_M for hydrolysis ($mM^{-1}min^{-1}$)	C/H ratio
SLP-wt	0.86	0.35	2.5
SLP-1	N/D	4.1	---
SLP-2	0.30	1.2	0.25
SLP-3	2.9	5.4	0.54
SLP-4	0.46	1.5	0.31
SLP-5	2.7	2.4	1.2
SLP-6	N/D	N/D	---
SLP-7	N/D	N/D	---

FIGURE 5: Results of Dap scan of **SLP-wt**. (A) Cyclic product of **SLP-wt**. The residues for which replacement by Dap results in neither cyclization nor hydrolysis are highlighted by shaded ovals. The residue for which replacement results in only hydrolysis is highlighted by a shaded square. The unhighlighted residues can be both cyclized and hydrolyzed when replaced by Dap. (B) HPLC traces of 1 h reactions initially containing 2 μM Srf TE, 500 μM indicated substrate, and 25 mM MOPS, at pH 7.0 and 24 °C. The peaks corresponding to the cyclic (C) and hydrolyzed (H) products, substrate (S), and enzyme (E) are labeled. The trace corresponding to **SLP-5** (labeled with asterisk) was run on a slower gradient than the other traces in order to achieve good peak separation. The identities of the substrates and products were verified by MALDI-TOF MS and/or LC-MS (Table 1). (C) The ratio of cyclization to hydrolysis (C/H ratio), and k_{cat}/K_M values of cyclization and hydrolysis, for each substrate (standard deviation ± 10%). N/D = activity not detected.

although the k_{cat}/K_M for hydrolysis increased even more, with a cyclization:hydrolysis ratio of 0.54:1 (Figure 5C). Qualitatively, this increase appeared to be due mainly to an increase in k_{cat}. To assess each of the mutant enzymes with a more active substrate, the activity of each was measured with **SLP-3**. While the catalytic triad mutants (S80C, D107A, H207A) continued to be inactive, the K111A mutant, which showed no measurable activity with **SLP-wt**, did show a low level of hydrolysis activity with **SLP-3** (Figure 4B).

Spacer Scan. A residue scan orthogonal to the Dap scan was also performed, in which two adjacent residues at a time, from Glu_1 to D-Leu_6, were replaced by the flexible spacer ε-aminohexanoic acid (ε-Ahx), to address which residue side chains are necessary for productive substrate positioning in the enzyme active site (Figure 6). We determined kinetic

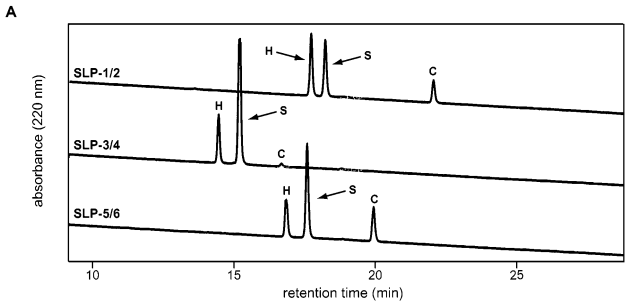

B

	k_{cat}/K_M for cyclization ($mM^{-1}min^{-1}$)	k_{cat}/K_M for hydrolysis ($mM^{-1}min^{-1}$)	C/H ratio
SLP-wt	0.86	0.35	2.5
SLP-1/2: FA-ε-Ahx-D-Leu_3-Val_4-Asp_5-D-Leu_6-Leu_7-SNAC	0.84	2.1	0.39
SLP-3/4: FA-Glu_1-Leu_2-ε-Ahx-Asp_5-D-Leu_6-Leu_7-SNAC	0.087	1.5	0.057
SLP-5/6: FA-Glu_1-Leu_2-D-Leu_3-Val_4-ε-Ahx-Leu_7-SNAC	1.4	1.4	1.0

FIGURE 6: Results of spacer scan of **SLP-wt**. (A) HPLC traces of 2 h reactions initially containing 2 μM Srf TE, 500 μM indicated substrate, and 25 mM MOPS, at pH 7.0 and 24 °C. The peaks corresponding to the cyclic (C) and hydrolyzed (H) products and substrate (S) are labeled. The identities of the substrates and products were verified by LC-MS (Table 1). (B) The ratio of cyclization to hydrolysis (C/H ratio), and k_{cat}/K_M values of cyclization and hydrolysis, for each substrate (standard deviation ± 10%). FA: (*R*)-3-hydroxybutyric acid.

parameters and cyclization:hydrolysis ratios of Srf TE on each substrate, and found that, unlike in the Dap scan, the removal of residue side chains toward the N- (**SLP-1/2**) and C-terminus (**SLP-5/6**) of the substrate did not dramatically affect the cyclization:hydrolysis ratios of the resulting substrates. In contrast, the removal of residue side chains in the middle of the substrate (**SLP-3/4**) resulted in significantly decreased cyclization by Srf TE, with a cyclization:hydrolysis ratio of 0.057:1 (Figure 6). These divergent results highlight the different substrate recognition properties probed in the two scans.

Reverse Reaction: Hydrolysis of the Cyclic Macrolactone. The cyclic macrolactone product of **SLP-wt** was also a substrate for Srf TE, with the enzyme reopening the macrolactone at the ester bond and catalyzing the formation of the linear acid through water attack (Figure 7). The k_{cat}/K_M for this hydrolysis was 0.40 mM^{-1} min^{-1}. In addition, the acyl-enzyme intermediate could also be captured through nucleophilic attack by ONAC, SNAC, or NNAC, with the resulting formation of linear esters, thioesters, or amides of the substrate, respectively (Figure 7C). As expected, the presence of exogenously added macrolactone inhibited the cyclization of SNAC thioester substrates in a concentration-dependent manner (data not shown).

Alterations to Leaving Group, Nucleophile, and Length of Substrate. The ability of Srf TE to reopen the macrolactone product suggested that it might cyclize linear peptide esters in addition to thioesters. The thioester of **SLP-wt** was therefore changed to an ester through the replacement of the SNAC with ONAC. Srf TE was able to both cyclize and hydrolyze the resulting substrate (**SLP−ONAC**), with a cyclization:hydrolysis ratio of 0.60:1 (Figure 8B), although the reaction occurred 5−10 times more slowly (data not shown). These results showed that Srf TE is able to tolerate

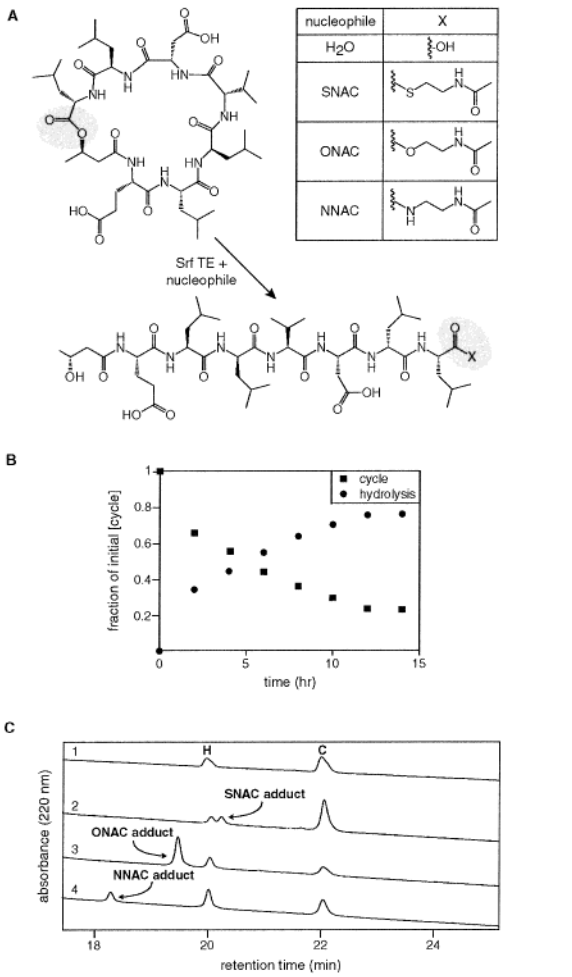

FIGURE 7: Enzymatic opening of macrolactone by Srf TE with different nucleophiles. (A) Mechanism of macrolactone opening. Srf TE can catalyze the attack of water or competing nucleophiles such as SNAC, ONAC, or NNAC to open the cyclic ester bond. (B) Time course (14 h) of hydrolysis of the cyclic product of **SLP-wt** by Srf TE, with time points taken every 2 h. (C) HPLC traces of 2 h reactions initially containing 2.5 μM Srf TE, 250 μM cyclic product of **SLP-wt**, 25 mM MOPS, at pH 7.0 and 24 °C. Each reaction also contained 250 mM of the following nucleophile: (1) none, (2) SNAC, (3) ONAC, (4) NNAC. The peaks corresponding to the cyclic substrate (C), hydrolyzed product (H), and product resulting from attack by the added nucleophile are labeled. The identities of the substrate and products were verified by MALDI-TOF MS (Table 1). SNAC adduct $[M - H]^-$, observed mass 999.0 (calculated mass 999.5); ONAC adduct $[M - H]^-$, 983.0 (983.5); NNAC adduct $[M - H]^-$, 981.9 (981.5).

a less active oxo leaving group in addition to the native thiol leaving group.

Variations were also made to the nucleophile-containing fatty acid of **SLP-3**, as summarized in Figure 9A. The heptapeptide of **SLP-3** was used instead of that of **SLP-wt**, because its greater solubility in water allowed for easier synthesis and purification of the multiple alternate substrates. A substrate in which a β-amino group was substituted for the secondary β-hydroxyl group of the fatty acid (**SLP−NH_2**) was not cyclized by Srf TE, although it was hydrolyzed (data not shown). Similar results were obtained on **(*R*)-** and **(*S*)-SLP-αOH**, which have a fatty acid containing a secondary α-hydroxyl group rather than a β-hydroxyl group, and also on a substrate in which the fatty acid was replaced by a serine (**SLP−Ser**), which contains primary β-hydroxyl and α-amino groups. On the other hand, a substrate with a fatty

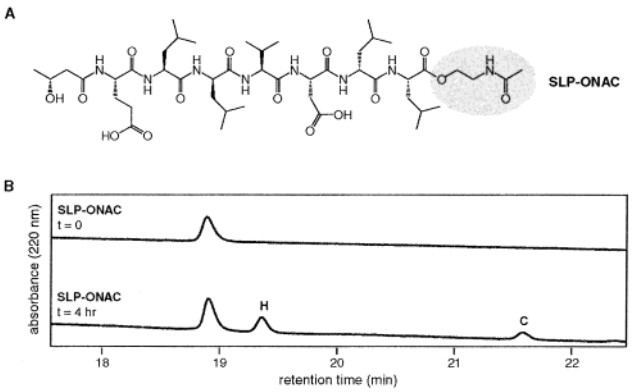

FIGURE 8: Cyclization and hydrolysis of peptide-ONAC ester substrate by Srf TE domain. (A) Structure of **SLP−ONAC**. (B) HPLC traces of 4 h reaction initially containing 2.5 μM Srf TE, 200 μM **SLP−ONAC**, and 25 mM MOPS, at pH 7.0 and 24 °C. The peaks corresponding to the cyclic (C) and hydrolyzed (H) products are labeled. The identities of the substrate and products were verified by MALDI-TOF MS (Table 1).

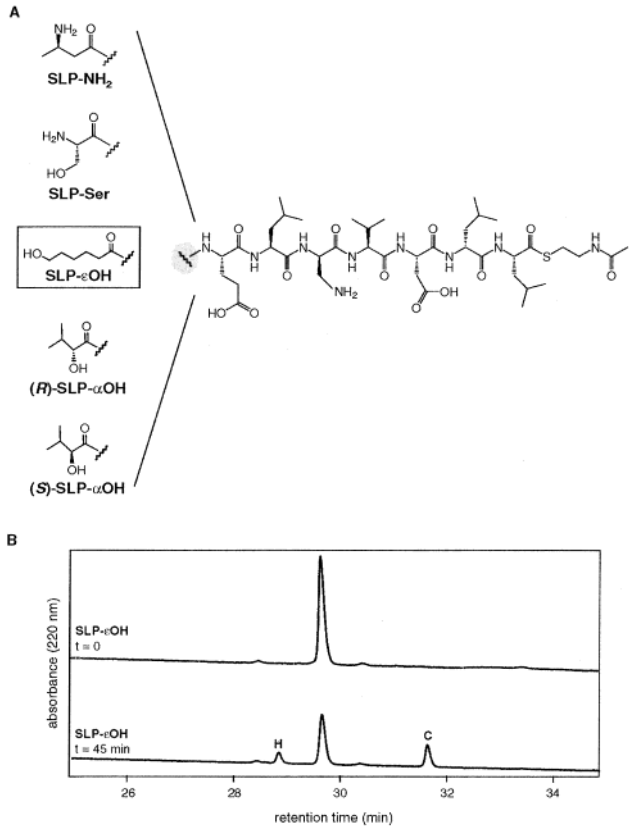

FIGURE 9: Variations to the nucleophilic attacking group of **SLP-3**. (A) The (*R*)-3-hydroxybutyric acid group was replaced by those shown. The altered substrate that could be cyclized by Srf TE, **SLP-ϵOH**, is boxed. (B) HPLC traces of 2 h reaction initially containing 2.5 μM Srf TE, 250 μM **SLP-ϵOH**, and 25 mM MOPS, at pH 7.0 and 24 °C. The peaks corresponding to the cyclic (C) and hydrolyzed (H) products are labeled. The identities of the substrate and products were verified by MALDI-TOF MS, and the cyclic product was additionally confirmed by HPLC MS-MS analysis.

acid containing a primary ϵ-hydroxyl group (**SLP-ϵOH**) was accepted as a substrate for both cyclization and hydrolysis, with a cyclization:hydrolysis ratio of 1.7:1, a k_{cat}/K_M for cyclization of 11 mM^{-1} min^{-1}, and a k_{cat}/K_M for hydrolysis of 6.3 mM^{-1} min^{-1} (Figure 9B). These initial data indicate that altered macrolactone ring size is possible. To further test this possibility, a nonapeptide version of **SLP-wt** was synthesized, with a Leu inserted between Leu_2 and D-Leu_3 and another between Val_4 and Asp_5. However, similar to **SLP−NH$_2$**, this substrate was hydrolyzed but not cyclized by Srf TE (data not shown). In addition, structurally unrelated peptidyl-SNAC substrates, including those with the peptide sequences of mycosubtilin (heptapeptide), fengycin (decapeptide), and tyrocidine (decapeptide), also showed substantial hydrolysis but no cyclization with Srf TE, indicating the enzyme's broad tolerance for hydrolysis but not cyclization of these longer substrates (data not shown).

Cocrystal Structures of Srf TE with Dipeptidyl Boronate Inhibitor. To further characterize the binding mode of surfactin linear peptides, we examined X-ray crystal structures of Srf TE bound to designed inhibitor molecules. A variety of linear peptides containing the surfactin heptapeptide sequence and a C-terminal boronic acid in place of the carboxyl group were synthesized using established procedures (*10*, *11*). Boronic acid-based inhibitors are widely used as potent inhibitors of serine proteases and esterases. The boronic acid moiety alkylates the catalytic serine, forming a tetrahedral boronate that closely mimics the tetrahedral intermediate in the reaction pathway. Peptides were soaked into crystals of Srf TE, and the structures were solved by molecular replacement using the structure of Srf TE (*8*). Peptide electron density was only clearly present for D-Leu_6, Leu_7, and the boronic acid group, irrespective of the length of the peptide used in the soaking experiment. The remaining residues of the substrate peptide were not well ordered in the maps. Figure 10 shows the structure of the enzyme bound to the dipeptide analogue *N*-acetyl-D-Leu-Leu-$B(OH)_2$ ($K_i = 50$ μM), and is representative of the observed electron density with full-length heptapeptide boronic acid analogues. The structure shows a tetrahedral boron atom bound both to the hydroxyl side chain of Ser80 and N3 of His270, a bidentate binding mode sometimes observed in serine protease/boronic acid complexes (*14*, *15*). The C-terminal Leu (corresponding to Leu_7) is bound specifically in a pocket adjacent to the triad, forming contacts with residues Tyr156, Tyr159, and Leu129. The D-Leu residue (corresponding to D-Leu_6) is also well ordered in the density maps, bound in a hydrophobic pocket consisting of Tyr109, Leu187, and Phe181. The *N*-acetyl group, corresponding to Asp_5 of the linear surfactin peptide, points out of the active-site pocket into bulk solvent.

DISCUSSION

The TE domain of surfactin synthetase catalyzes the cyclization of linear β-hydroxy-acyl-heptapeptidyl thioesters and esters to produce cyclic macrolactones through the capture of the Leu_7 carbonyl by the fatty acyl β-hydroxyl nucleophile (Figure 2B). This is representative of the terminal step in the biosynthesis of other cyclic peptidolactones, including globomycin (*16*) and tripropeptin (*17*), and analogous peptidolactams, such as the iturins (*18*). The related nonribosomal peptidolactones in the daptomycin (*19*) and ramoplanin (*4*) classes of antibiotics are similarly macrocyclized at the end of the NRPS assembly line by TE domains that use as the cyclization nucleophile a β-hydroxyl group of an amino acid side chain instead of a fatty acid. To evaluate the catalytic capabilities of these cyclic depsipeptide synthases, we have characterized active-site mutants of Srf TE for cyclization and thioester hydrolysis activity. We have

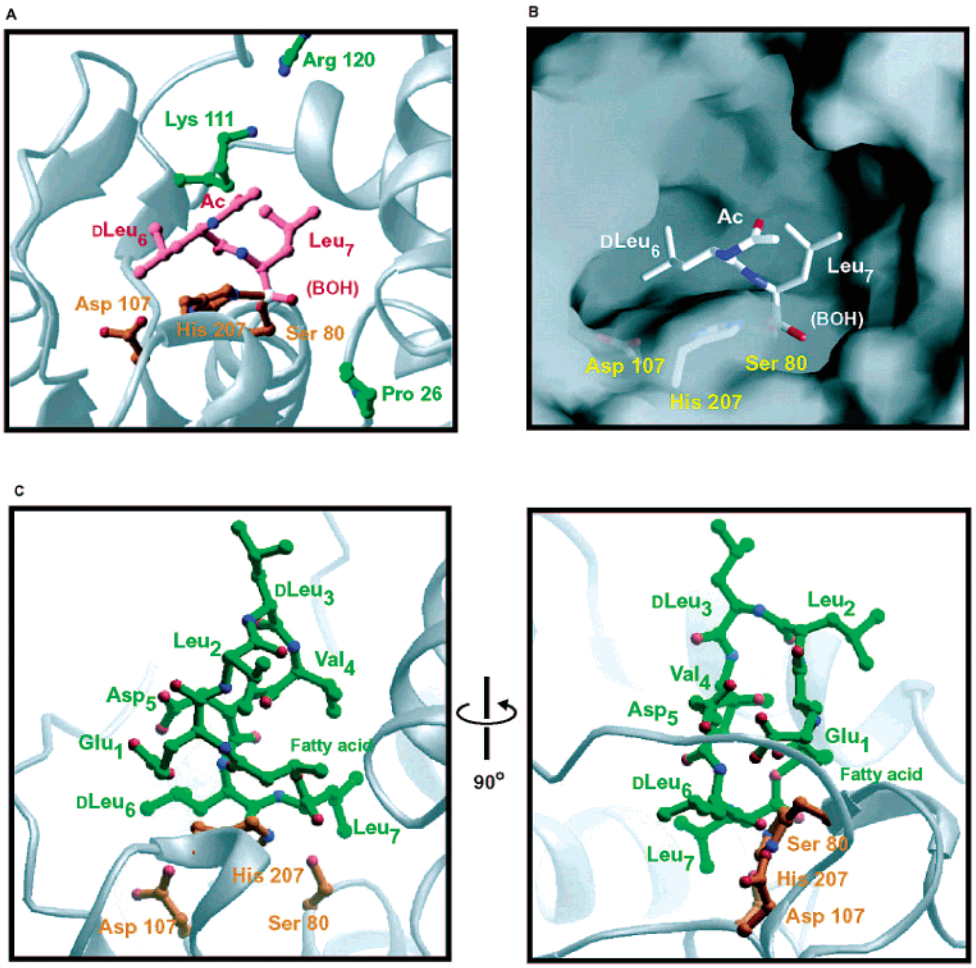

FIGURE 10: X-ray crystal structure of Srf TE bound to a dipeptide boronic acid analogue. (A) Structure of *N*-acetyl-D-Leu-Leu-B(OH)$_2$ complexed to Srf TE. The dipeptide analogue is shown in pink, the catalytic triad in yellow, and additional active-site side chains in green. (B) Surface representation of the active-site pocket in the same orientation as in part A, with *N*-acetyl-D-Leu-Leu-B(OH) and the catalytic triad in licorice representation. (C) Model of the cyclizing conformation of the surfactin linear peptide. Superposition of the NMR structure of surfactin onto the structure of *N*-acetyl-D-Leu-Leu-B(OH) in the active site. The first panel is in the same orientation as in parts A and B; the second panel is rotated 90° to illustrate the β-sheet structure of the conform.

also begun an assessment of the contributions of the fatty acyl group, heptapeptide backbone, and leaving group to substrate recognition for both cyclization and hydrolysis.

The superfamily of serine esterases generally uses a catalytic triad of active-site residues, with serine as nucleophile, histidine as acid/base catalyst, and aspartate to orient the histidine and serine residues optimally (*20*). Mutational analysis on the chicken FAS TE domain (*21*) and enterobactin synthetase TE domain (*22*) validated the roles of the active-site serine and histidine. In the enterobactin system, the Ser→Cys mutant showed a 1000-fold decrease in activity compared with the wild-type enzyme, and the His→Ala mutant showed a 10000-fold decrease (*22*). The X-ray structure of the Srf TE domain indicated that Ser80, His207, and Asp107 were architecturally disposed to be such a catalytic triad (*8*). Mutagenesis results reported here verify that the S80C and H207A mutants were without detectable activity in both cyclization and hydrolysis assays, with the D107A mutant also showing no cyclization activity and only a trace amount of hydrolysis activity.

In acyl-*O*-Ser enzyme intermediate formation and breakdown, anionic tetrahedral adducts are predicted, and electrostatic stabilization via oxyanion hole interaction is a general tenet of the superfamily catalytic mechanism (*20*). For Srf TE, the backbone amides of Ala81 and Val27 are thought to serve this function (Figure 10A) (*8*). We have focused on Pro26 just adjacent to Val27, since it is a conserved residue in NRPS TE domains, but is instead conserved as a glycine in the lipase subfamily of serine esterases, which carry out acyl transfer exclusively to water as the nucleophilic cosubstrate. In fact, the P26G Srf TE mutant had a 13-fold increase in k_{cat}/K_M, with a 12-fold change in product partition ratio away from intramolecular cyclization in favor of intermolecular hydrolysis. The change from a rigid proline to a flexible glycine may increase the conformational freedom in this region of the active site and create more access for water or its productive orientation for capture of the acyl-heptapeptidyl-*O*-Ser enzyme intermediate. In turn, it may be that mutation of lipase active sites to introduce the proline may enhance intramolecular cyclization outcomes.

One of the goals of this study was to evaluate features in substrates that allow the excised Srf TE to carry out the chemo-, regio-, and stereospecific macrocyclization to the lariat type of peptidolactone, as prelude to evaluation of its catalytic potential for biogenesis of novel macrocyclic products. A significant limitation in our initial study was the poor aqueous solubility of the fatty acyl-heptapeptidyl-

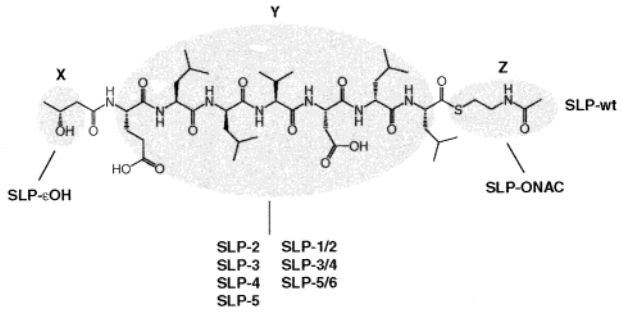

FIGURE 11: Summary of alternate substrates tolerated by Srf TE. In this study, different parts (X, Y, and Z) of a peptidyl-SNAC thioester substrate (**SLP-wt**) were altered. (X) Nucleophilic attacking group of fatty acid, (Y) heptapeptide sequence, (Z) leaving group. The listed substrates could be cyclized by Srf TE.

SNAC thioesters (*1*). As a result, we shortened the acyl chain from the natural $C_{13}-C_{15}$ length down to C_4, and introduced an ornithine side chain as a solubilizing element. In this work, we retained the β-hydroxybutyric acid for ease of synthesis, purification, and assay, but will need to explore in the future how longer fatty acyl chains may affect catalytic efficiency. Even with the C_4 acyl chain, solubility in water was low, creating problems in kinetic assays. We tried to increase solubility by systematically introducing a Dap residue at each of the seven positions of the heptapeptide sequence of surfactin. The substrate with Dap at the third position (**SLP-3**) was more tractable than the substrate with the wild-type heptapeptide sequence (**SLP-wt**), but was still not optimal for deconvolution of k_{cat} and K_M values.

Nonetheless, HPLC assays could be performed on all of the substrates and relative rates of cyclization and hydrolysis determined (Figure 5C). Both the intermolecular hydrolysis and intramolecular cyclization reactions were enzyme-mediated and are presumed to reflect competing fates for deacylation of the acyl-heptapeptidyl-*O*-TE enzyme intermediate (Figure 2B). Some structure/activity data for TE action were acquired on the nucleophile (X) in the acyl moiety, determinants in the heptapeptide chain (Y), and leaving group (Z), as highlighted in Figure 11.

For the C_4 acyl chain, when X = OH, the peptidolactone could be formed by macrocyclization, while when $X = NH_2$, only hydrolysis occurred. It is possible that this outcome may be altered for longer acyl chains, since the β-NH_2 group of a C_{14-17} acyl chain is the cyclizing nucleophile in the closely related iturin peptidolactam antibiotic (*18*). When the attacking hydroxyl group of the acyl chain was moved from the β- to α-position, only hydrolysis occurred, suggesting misalignment or steric barriers to intramolecular lactonization. However, the straight chain ϵ-hydroxycaproyl chain was cyclized to generate a peptidolactone with three more carbon atoms, suggesting further exploration of ω-hydroxy-acylpeptidyl substrates may be useful.

In terms of alteration of the heptapeptide backbone, Y, lengthening to the nonamer gave hydrolysis but no cyclization, as though a cyclizing conformer in the active site were disfavored. The Dap scan, in which each side chain was replaced with one that differed in both size and charge, indicated tolerance of Dap in the middle of the peptidyl chain, but not at the N- or C-terminus, in some analogy to the tolerance of the tyrocidine synthetase TE domain (TycC TE) to treat internal residues in a cyclizing chain as substitutable cargo (Figure 5) (*1*, *3*). The failure of some Dap substrates to cyclize (**SLP-1**), or both hydrolyze and cyclize (**SLP-6**/**SLP-7**), indicated a rejection of the attempted change rather than a requirement for the wild-type side chain. On the other hand, the spacer scan, which replaced pairs of adjacent residues with a minimal linker containing no peptide bonds or side chains, probed the requirement for such side chains, as well as the peptide bonds between them. The results of the spacer scan indicated that, while the residues toward the N- or C-terminus of the substrate are not tolerant to significant side-chain changes, the presence of residues at either end is not necessary for cyclization. In contrast, the removal of residues in the middle of the substrate had a marked effect on cyclization (Figure 6). In combination with the findings from the Dap scan, this suggests that the peptide backbone of the middle residues is an important feature for cyclization of the substrate.

The leaving group, Z, is an *S*-phosphopantetheinyl chain covalently tethered to the T domain of the SrfC subunit in the native environment of the surfactin synthetase assembly line (Figure 2B). This macromolecular portion of the substrate can be replaced by an SNAC thioester in this and other assembly line TE domains, albeit with some loss of affinity. Changing from a thiol to hydroxyl leaving group still retained sufficient thermodynamic activation in the substrate for Srf TE-mediated cyclization (Figure 8). In the cognate TycC TE case, we have used such oxoester chemistry to make peptide libraries on beads to allow facilitated screening of libraries that can be enzymatically cyclized (*23*). In addition, Srf TE also catalyzes the reverse reaction, the peptidolactone ring opening, where the leaving group is the β-hydroxyl group of the acyl chain (Figure 7).

While the expected acylheptapeptidyl-*O*-TE intermediate has yet to be isolated, e.g., in rapid quench studies, the cocrystallization of the D-Leu-Leu-boronate with the boron bridging Ser80 and His207 is consistent with the mechanistic prediction for the catalytic pathway (Figure 10A). In agreement with biochemical data, only the peptide side chains of D-Leu_6 and Leu_7 show specific binding in the active-site pocket, each bound tightly in a well-defined hydrophobic pocket. These two amino acids fill up most of the active site, with the remainder of the peptide chain jutting out of the pocket (Figure 10). Starting from this orientation of residues 6 and 7 of the heptapeptidyl chain and the NMR structure of the cyclic surfactin product (*24*), one can model the full heptapeptidyl chain in a product-like conformer as prelude to subsequent structure/activity/engineering mutagenesis on Srf TE and, by extension, other macrocyclizing NRPS TE domains. This model sets the surfactin linear peptide in a twisted β-sheet structure pointing away from the active-site pocket into solution (Figure 10C). Consistent with the substrate tolerance of Srf TE, the enzyme makes specific contacts only with the two termini of the linear peptide. The proximity of the fatty acid of the natural surfactin linear lipopeptide to the nucleophilic hydroxyl group may suggest that it is a necessary determinant for cyclization. A pronounced hydrophobic pocket is present in the active site close to the predicted fatty acid position and may assist in increasing cyclization to hydrolysis product distribution.

Further comparison of Srf TE to TycC TE and other macrolactonizing and macrolactamizing TE domains, excised from both NRPS and PKS assembly lines, is warranted to

sort out the determinants of intramolecular cyclization vs intermolecular hydrolysis for the acyl-*O*-TE intermediates. For example, Srf TE makes a branched chain peptidolactone, utilizing a D-hydroxyl stereocenter in the intramolecular nucleophile. TycC TE also uses a D-stereocenter in the attacking nucleophile, but it is an amine nucleophile and the product is a head-to-tail cyclized macrolactam. Minimal substrate recognition by TycC TE appears to consist only of an N-terminal D-phenylalanine and penultimate ornithine, and the potential of the substrate to preorganize into an antiparallel β-sheet, with multiple residue substitutions and length variations well tolerated (*1*, *3*, *25*). In contrast, our analysis of Srf TE indicates that it is optimized for its naturally dedicated substrate, with catalysis of cyclization only retained by conservative changes to the substrate sequence. Deciphering the productive folding of acyclic conformers of the acyl chain in the binding pockets of acyl-*O*-TE intermediates will be crucial in future studies to understand cyclization vs hydrolysis outcomes.

ACKNOWLEDGMENT

We would like to thank Dr. Milton T. Stubbs for advice on structural and mechanistic analysis, the Verdine lab for use of crystallographic facilities, and members of the Walsh lab for helpful discussions.

REFERENCES

1. Kohli, R. M., Trauger, J. W., Schwarzer, D., Marahiel, M. A., and Walsh, C. T. (2001) *Biochemistry 40*, 7099−7108.
2. Schwarzer, D., and Marahiel, M. A. (2001) *Naturwissenschaften 88*, 93−101.
3. Trauger, J. W., Kohli, R. M., and Walsh, C. T. (2001) *Biochemistry 40*, 7092−7098.
4. Skelton, N. J., Harding, M. M., Mortishire-Smith, R. J., Rahman, S. K., Williams, D. H., Rance, M. J., and Ruddock, J. C. (1991) *J. Am. Chem. Soc. 113*, 7522−7530.
5. Peypoux, F., Bonmatin, J. M., and Wallach, J. (1999) *Appl. Microbiol. Biotechnol. 51*, 553−563.
6. Cosmina, P., Rodriguez, F., de Ferra, F., Grandi, G., Perego, M., Venema, G., and van Sinderen, D. (1993) *Mol. Microbiol. 8*, 821−831.
7. Stein, T., Vater, J., Kruft, V., Otto, A., Wittmann-Liebold, B., Franke, P., Panico, M., McDowell, R., and Morris, H. R. (1996) *J. Biol. Chem. 271*, 15428−15435.
8. Bruner, S. D., Weber, T., Kohli, R. M., Schwarzer, D., Marahiel, M. A., Walsh, C. T., and Stubbs, M. T. (2002) *Structure 10*, 301−310.
9. Trauger, J. W., Kohli, R. M., Mootz, H. D., Marahiel, M. A., and Walsh, C. T. (2000) *Nature 407*, 215−218.
10. Martichonok, V., and Jones, J. B. (1996) *J. Am. Chem. Soc. 118*, 950−958.
11. Coutts, S. J., Adams, J., Krolikowski, D., and Snow, R. J. (1994) *Tetrahedron Lett. 35*, 5109−5112.
12. Wong, H., and Schotz, M. C. (2002) *J. Lipid Res. 43*, 993−999.
13. Osman, M., Ishigami, Y., Ishikawa, K., Ishizuka, Y., and Holmsen, H. (1994) *Biotechnol. Lett. 16*, 913−918.
14. Stoll, V. S., Eger, B. T., Hynes, R. C., Martichonok, V., Jones, J. B., and Pai, E. F. (1998) *Biochemistry 37*, 451−462.
15. Takahashi, L. H., Radhakrishnan, R., Rosenfield, R. E., Jr., and Meyer, E. F., Jr. (1989) *Biochemistry 28*, 7610−7617.
16. Kogen, H., Kiho, T., Nakayama, M., Furukawa, Y., Kinoshita, T., and Inukai, M. (2000) *J. Am. Chem. Soc. 122*, 10214−10215.
17. Hashizume, H., Igarashi, M., Hattori, S., Hori, M., Hamada, M., and Tageuchi, T. (2001) *J. Antibiot. 54*, 1054−1059.
18. Tsuge, K., Akiyama, T., and Shoda, M. (2001) *J. Bacteriol. 183*, 6265−6273.
19. Debono, M., Abbott, B. J., Molloy, R. M., Fukuda, D. S., Hunt, A. H., Daupert, V. M., Counter, F. T., Ott, J. L., Carrell, C. B., Howard, L. C., Boeck, L. D., and Hamill, R. L. (1988) *J. Antibiot. 41*, 1093−1105.
20. Kraut, J. (1977) *Annu. Rev. Biochem. 46*, 331−358.
21. Pazirandeh, M., Chirala, S. S., and Wakil, S. J. (1991) *J. Biol. Chem. 266*, 20946−20952.
22. Shaw-Reid, C. A., Kelleher, N. L., Losey, H. C., Gehring, A. M., and Walsh, C. T. (1999) *Chem. Biol. 6*, 385−400.
23. Kohli, R. M., Walsh, C. T., and Burkart, M. D. (2002) *Nature 418*, 658−661.
24. Bonmatin, J.-M., Genest, M., Labbé, H., and Ptak, M. (1994) *Biopolymers 34*, 975−896.
25. Kohli, R. M., Takagi, J., and Walsh, C. T. (2002) *Proc. Natl. Acad. Sci. U.S.A. 99*, 1247−1252.

BI026592A